

Quark deconfinement phase transition in neutron stars

Grigor Alaverdyan
Department of Radiophysics
Chair of Wave Processes Theory
Yerevan State University
Yerevan 0025
Armenia
Email: galaverdyan@ysu.am

Abstract

The hadron-quark phase transition in the interior of compact stars is investigated, when the transition proceeds through a mixed phase. The hadronic phase is described in the framework of relativistic mean-field theory, when also the scalar-isovector delta-meson mean-field is taken into account. The changes of the parameters of phase transition caused by the presence of delta-meson field are explored. The results of calculation of structure of the mixed phase (Glen-denning construction) are compared with the results of usual first-order phase transition (Maxwell construction).

Key words: neutron stars: quarks: phase transition: mixed phase

PACS numbers: 97.60.Jd, 26.60.+c, 12.39.Ba

1 Introduction

The structure of compact stars functionally depends on the equation of state (EOS) of matter in a sufficiently wide range of densities - from 7.9 g/cm^3 (the endpoint of thermonuclear burning) to one order of magnitude higher than nuclear saturation density. Therefore, the study of properties and composition of the matter constituents at extremely high density region is of a great interest in both nuclear and neutron star physics. The relativistic mean-field (RMF) theory [1, 2, 3] has been effectively applied to describe the structure of finite nuclei[4, 5], the features of heavy-ion collisions[6, 7], and the equation of state (EOS) of nuclear matter[8]. Inclusion of the scalar-isovector δ -meson in this theoretical scheme and investigation of its influence on low density asymmetric nuclear matter was realized in Refs.[9, 10, 11]. At sufficiently high density, different exotic degrees of freedom, such as pion and kaon condensates, also

deconfined quarks, may appear in the strongly interacting matter. The modern concept of hadron-quark phase transition is based on the feature of that transition, that is the presence of two conserved quantities in this transition: baryon number and electric charge[12]. It is known that, depending on the value of surface tension, σ_s , the phase transition of nuclear matter into quark matter can occur in two scenarios [13]: ordinary first order phase transition with a density jump (Maxwell construction), or formation of a mixed hadron-quark matter with a continuous variation of pressure and density (Glendenning construction)[12]. Uncertainty of the surface tension values does not allow to determine the phase transition scenario, taking place in reality. In our recent paper [14] in the assumption that the transition to quark matter is a usual first-order phase transition, described by Maxwell construction, we have shown that the presence of the δ -meson field leads to the decrease of transition pressure P_0 , of baryon number densities n_N and n_Q . In this article we investigate the hadron-quark phase transition of neutron star matter, when the transition proceeds through a mixed phase. The results of calculation of structure of the mixed phase(Glendenning construction) are compared with the results of usual first-order phase transition (Maxwell construction). Influence of δ -meson field on phase transition characteristics is discussed. Finally, using the EOS obtained, we calculate the integral and structural characteristics of Neutron stars with quark degrees of freedom.

2 Neutron star matter equation of state

2.1 Nuclear matter

In this section we consider the EOS of matter in the region of nuclear and supranuclear density($n \geq 0.1 \text{ fm}^{-3}$). For the lower density region, corresponding to the outer and inner crust of the star, we have used the EOS of Baym-Bethe-Pethick (BBP)[15]. For description of hadronic phase we use the relativistic Lagrangian density of many-particle system consisted of nucleons, p , n , and isoscalar-scalar (σ), isoscalar-vector (ω), isovector-scalar (δ), and isovector-vector (ρ) - exchanged mesons :

$$\mathcal{L}_{\sigma\omega\rho\delta}(\sigma(x), \omega_\mu(x), \vec{\rho}_\mu(x), \vec{\delta}(x)) = \mathcal{L}_{\sigma\omega\rho}(\sigma(x), \omega_\mu(x), \vec{\rho}_\mu(x)) - U(\sigma(x)) + \mathcal{L}_\delta(\vec{\delta}(x)), \quad (1)$$

where $\mathcal{L}_{\sigma\omega\rho}$ is the linear part of relativistic Lagrangian density without δ -meson field [16], $U(\sigma) = \frac{b}{3}m_N (g_\sigma\sigma)^3 + \frac{c}{4}(g_\sigma\sigma)^4$ is the σ -meson self-interaction term and

$$\mathcal{L}_\delta(\vec{\delta}) = g_\delta\bar{\psi}_N\vec{\tau}_N\vec{\delta}\psi_N + \frac{1}{2}(\partial_\mu\vec{\delta}\partial^\mu\vec{\delta} - m_\delta\vec{\delta}^2) \quad (2)$$

is the contribution of the δ -meson field. This Lagrangian density (1) contains the meson-nucleon coupling constants, g_σ , g_ω , g_ρ , g_δ and also parameters of σ -field self-interacting terms, b and c . In our calculations we take for the δ coupling constant,

$a_\delta = (g_\delta/m_\delta)^2 = 2.5 \text{ fm}^2$, as in [10, 11, 14], for the bare nucleon mass, $m_N = 938.93 \text{ MeV}$, for the nucleon effective mass, $m_N^* = 0.78 m_N$, for the baryon number density at saturation, $n_0 = 0.153 \text{ fm}^{-3}$, for the binding energy per baryon, $f_0 = -16.3 \text{ MeV}$, for the incompressibility modulus, $K = 300 \text{ MeV}$, and for the asymmetry energy, $E_{sym}^{(0)} = 32.5 \text{ MeV}$. Five other constants $a_\sigma = (g_\sigma/m_\sigma)^2$, $a_\omega = (g_\omega/m_\omega)^2$, $a_\rho = (g_\rho/m_\rho)^2$, b and c then can be numerically determined[14]. In Table 1 we list the

	a_σ (fm ²)	a_ω (fm ²)	a_δ (fm ²)	a_ρ (fm ²)	b (fm ⁻¹)	c
$\sigma\omega\rho$	9.154	4.828	0	4.794	$1.654 \cdot 10^{-2}$	$1.319 \cdot 10^{-2}$
$\sigma\omega\rho\delta$	9.154	4.828	2.5	13.621	$1.654 \cdot 10^{-2}$	$1.319 \cdot 10^{-2}$

Table 1: Model parameters without ($\sigma\omega\rho$) and with ($\sigma\omega\rho\delta$) a δ -meson field.

values of the model parameters with ($\sigma\omega\rho\delta$) and without ($\sigma\omega\rho$) the isovector-scalar δ meson interaction channel.

The knowledge of the model parameters makes it possible to solve the set of four equations in a self-consistent way and to determine the re-denoted mean-fields, $\sigma \equiv g_\sigma \bar{\sigma}$, $\omega \equiv g_\omega \bar{\omega}_0$, $\delta \equiv g_\delta \bar{\delta}^{(3)}$, and $\rho \equiv g_\rho \bar{\rho}_0^{(3)}$, depending on baryon number density n and asymmetry parameter $\alpha = (n_n - n_p)/n$. The standard QHD procedure allows to obtain expressions for energy density $\varepsilon(n, \alpha)$ and pressure $P(n, \alpha)$ of nuclear npe plasma:

$$\begin{aligned} \varepsilon_{NM}(n, \alpha, \mu_e) = & \frac{1}{\pi^2} \int_0^{k_-(n, \alpha)} \sqrt{k^2 + m_p^*(\sigma, \delta)^2} k^2 dk + \frac{1}{\pi^2} \int_0^{k_+(n, \alpha)} \sqrt{k^2 + m_n^*(\sigma, \delta)^2} k^2 dk \\ & + \frac{b}{3} m_N \sigma^3 + \frac{c}{4} \sigma^4 + \frac{1}{2} \left(\frac{\sigma^2}{a_\sigma} + \frac{\omega^2}{a_\omega} + \frac{\delta^2}{a_\delta} + \frac{\rho^2}{a_\rho} \right) \\ & + \frac{1}{\pi^2} \int_0^{\sqrt{\mu_e^2 - m_e^2}} \sqrt{k^2 + m_e^2} k^2 dk, \quad (3) \end{aligned}$$

$$\begin{aligned} P_{NM}(n, \alpha, \mu_e) = & \frac{1}{\pi^2} \int_0^{k_-(n, \alpha)} \left(\sqrt{k_-(n, \alpha)^2 + m_p^*(\sigma, \delta)^2} - \sqrt{k^2 + m_p^*(\sigma, \delta)^2} \right) k^2 dk \\ & + \frac{1}{\pi^2} \int_0^{k_+(n, \alpha)} \left(\sqrt{k_+(n, \alpha)^2 + m_n^*(\sigma, \delta)^2} - \sqrt{k^2 + m_n^*(\sigma, \delta)^2} \right) k^2 dk \\ & - \frac{b}{3} m_N \sigma^3 - \frac{c}{4} \sigma^4 + \frac{1}{2} \left(-\frac{\sigma^2}{a_\sigma} + \frac{\omega^2}{a_\omega} - \frac{\delta^2}{a_\delta} + \frac{\rho^2}{a_\rho} \right) \end{aligned}$$

$$+ \frac{1}{3\pi^2} \mu_e (\mu_e^2 - m_e^2)^{3/2} - \frac{1}{\pi^2} \int_0^{\sqrt{\mu_e^2 - m_e^2}} \sqrt{k^2 + m_e^2} k^2 dk, \quad (4)$$

where μ_e is the chemical potential of electrons,

$$m_p^*(\sigma, \delta) = m_N - \sigma - \delta, \quad m_n^*(\sigma, \delta) = m_N - \sigma + \delta \quad (5)$$

are the effective masses of the proton and neutron, respectively, and

$$k_{\pm}(n, \alpha) = \left(\frac{3\pi^2 n}{2} (1 \pm \alpha) \right)^{1/3}. \quad (6)$$

The chemical potentials of the proton and neutron are given by

$$\mu_p(n, \alpha) = \sqrt{k_F(n)^2 (1 - \alpha)^{2/3} + (m_N - \sigma - \delta)^2} + \omega + \frac{1}{2}\rho, \quad (7)$$

$$\mu_n(n, \alpha) = \sqrt{k_F(n)^2 (1 + \alpha)^{2/3} + (m_N - \sigma + \delta)^2} + \omega - \frac{1}{2}\rho. \quad (8)$$

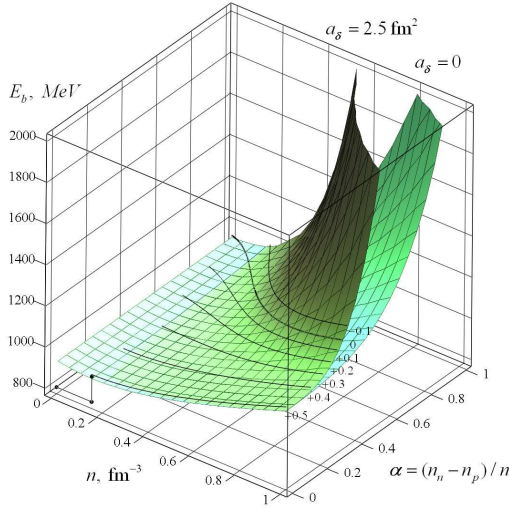


Figure 1: Energy per baryon E_b as a function of the baryon number density n and the asymmetry parameter α in case of a β -equilibrium charge neutral npe -plasma.

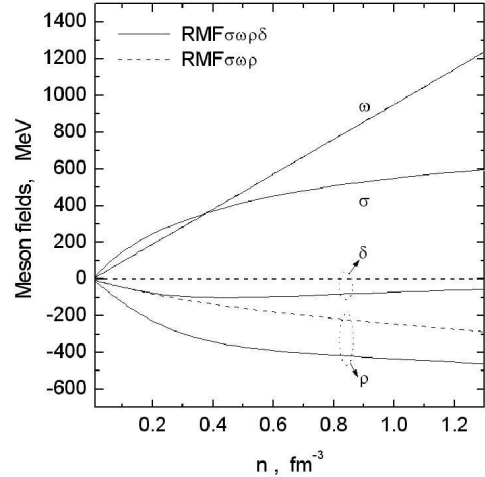


Figure 2: Re-denoted meson mean-fields as a function of the baryon number density n in case of a β -equilibrium charge neutral npe -plasma with and without δ -meson field.

In Fig 1 we illustrate the 3D-plot of the energy per baryon, $E_b(n, \alpha) = \varepsilon_{NM}/n$, as a function of the baryon number density n and asymmetry parameter α in case

of a β -equilibrium charged npe -plasma[17]. The curves correspond to different fixed values of the charge per baryon, $q = (n_p - n_e)/n = (1 - \alpha)/2 - n_e/n$. The thick one corresponds to β -equilibrium charge-neutral npe -matter. The lower and upper surfaces correspond to the " $\sigma\omega\rho$ " and " $\sigma\omega\rho\delta$ " models, respectively. Clearly, including a δ -meson field increases the energy per baryon, and this change is greater for larger values of the asymmetry parameter. For a fixed value of the specific charge, the asymmetry parameter falls off monotonically with the increase of density.

In Fig 2 we plotted the effective mean-fields of exchanged mesons, σ , ω , ρ and δ as a function of the baryon number density n for the charge-neutral β -equilibrium npe -plasma. The solid and dashed lines correspond to the " $\sigma\omega\rho\delta$ " and " $\sigma\omega\rho$ " models, respectively. From Fig 2 one can see that the inclusion of the scalar-isovector virtual $\delta(a_0(980))$ meson results in significant changes of ρ and δ meson fields. This can result in changes of deconfinement phase transition parameters and, thus, alter the structural characteristics of neutron stars.

The results of our analysis show that the scalar - isovector δ -meson field inclusion leads to the increase of the EOS stiffness of nuclear matter due to the splitting of proton and neutron effective masses, and also the increase of asymmetry energy (for details see Ref.[17]).

2.2 Quark matter

To describe the quark phase an improved version of the MIT bag model[18] is used, in which the interactions between u , d , s quarks inside the bag are taken into account in the one-gluon exchange approximation [19]. The quark phase consists of three quark flavors u , d , s and electrons in equilibrium with respect to weak interactions. We choose $m_u = 5$ MeV, $m_d = 7$ MeV and $m_s = 150$ MeV for quark masses and $\alpha_s = 0.5$ for the strong interaction constant.

2.3 Deconfinement phase transition parameters

There are two independent conserved charges in hadron-quark phase transition: baryonic charge and electric charge. The constituents chemical potentials of the npe -plasma in β -equilibrium are expressed through two potentials, $\mu_b^{(NM)}$ and $\mu_{el}^{(NM)}$, according to conserved charges, as follows

$$\mu_n = \mu_b^{(NM)}, \quad \mu_p = \mu_b^{(NM)} - \mu_{el}^{(NM)}, \quad \mu_e = \mu_{el}^{(NM)}. \quad (9)$$

In this case, the pressure P , energy density ε and baryon number density n , are functions of potentials, $\mu_b^{(NM)}$ and $\mu_{el}^{(NM)}$: $P_{NM}(\mu_b^{(NM)}, \mu_{el}^{(NM)})$, $\varepsilon_{NM}(\mu_b^{(NM)}, \mu_{el}^{(NM)})$, $n_{NM}(\mu_b^{(NM)}, \mu_{el}^{(NM)})$.

The particle species chemical potentials for *udse*-plasma in β -equilibrium are expressed through the chemical potentials $\mu_b^{(QM)}$ and $\mu_{el}^{(QM)}$ as follows

$$\begin{aligned}\mu_u &= \frac{1}{3} \left(\mu_b^{(QM)} - 2 \mu_{el}^{(QM)} \right), \\ \mu_d &= \mu_s = \frac{1}{3} \left(\mu_b^{(QM)} + \mu_{el}^{(QM)} \right), \\ \mu_e &= \mu_d - \mu_u = \mu_{el}^{(QM)}.\end{aligned}\tag{10}$$

In this case, the thermodynamic characteristics are functions of chemical potentials $\mu_b^{(QM)}$ and $\mu_{el}^{(QM)}$: $P_{QM}(\mu_b^{(QM)}, \mu_{el}^{(QM)})$, $\varepsilon_{QM}(\mu_b^{(QM)}, \mu_{el}^{(QM)})$, $n_{QM}(\mu_b^{(QM)}, \mu_{el}^{(QM)})$.

The mechanical and chemical equilibrium conditions (Gibbs conditions) for mixed phase are

$$\mu_b^{(QM)} = \mu_b^{(NM)} = \mu_b, \quad \mu_{el}^{(QM)} = \mu_{el}^{(NM)} = \mu_{el},\tag{11}$$

$$P_{QM}(\mu_b, \mu_{el}) = P_{NM}(\mu_b, \mu_{el}).\tag{12}$$

The volume fraction of quark phase is

$$\chi = V_{QM} / (V_{QM} + V_{NM}),\tag{13}$$

where V_{QM} and V_{NM} are volumes occupied by quark matter and nucleonic matter, respectively.

We applied the global electrical neutrality condition for mixed quark-nucleonic matter, according to Glendenning [12, 16],

$$\begin{aligned}& (1 - \chi) [n_p(\mu_b, \mu_{el}) - n_e(\mu_{el})] \\ + \chi \left[\frac{2}{3} n_u(\mu_b, \mu_{el}) - \frac{1}{3} n_d(\mu_b, \mu_{el}) - \frac{1}{3} n_s(\mu_b, \mu_{el}) - n_e(\mu_{el}) \right] &= 0.\end{aligned}\tag{14}$$

The baryon number density in the mixed phase is determined as

$$\begin{aligned}n &= (1 - \chi) [n_p(\mu_b, \mu_{el}) + n_n(\mu_b, \mu_{el})] \\ + \frac{1}{3} \chi [n_u(\mu_b, \mu_{el}) + n_d(\mu_b, \mu_{el}) + n_s(\mu_b, \mu_{el})],\end{aligned}\tag{15}$$

and the energy density is

$$\begin{aligned}\varepsilon &= (1 - \chi) [\varepsilon_p(\mu_b, \mu_{el}) + \varepsilon_n(\mu_b, \mu_{el})] \\ + \chi [\varepsilon_u(\mu_b, \mu_{el}) + \varepsilon_d(\mu_b, \mu_{el}) + \varepsilon_s(\mu_b, \mu_{el})] + \varepsilon_e(\mu_{el}).\end{aligned}\tag{16}$$

In case of $\chi = 0$, the chemical potentials μ_b^N and μ_{el}^N corresponding to the lower threshold of a mixed phase, are determined by solving Eqs. (12) and (14). This allows to determine the lower boundary parameters P_N , ε_N and n_N . Similarly, we determine the upper boundary values of mixed phase parameters, P_Q , ε_Q and n_Q , for

Model	n_N (fm ⁻³)	n_Q (fm ⁻³)	P_N (MeV/fm ³)	P_Q (MeV/fm ³)	ε_N (MeV/fm ³)	ε_Q (MeV/fm ³)
B60 $\sigma\omega\rho$	0.0717	1.083	0.336	327.747	67.728	1280.889
B60 $\sigma\omega\rho\delta$	0.0771	1.083	0.434	327.745	72.793	1280.884
B100 $\sigma\omega\rho$	0.2596	1.436	18.025	471.310	253.814	1870.769
B100 $\sigma\omega\rho\delta$	0.2409	1.448	16.911	474.368	235.029	1889.336

Table 2: The Mixed phase threshold parameters without ($\sigma\omega\rho$) and with ($\sigma\omega\rho\delta$) a δ -meson field for bag parameter values, $B = 60$ MeV/fm³ and $B = 100$ MeV/fm³.

$\chi = 1$. The system of Eqs. (12), (14),(15) and (16) makes it possible to determine EOS of mixed phase between this critical states.

Note, that in the case of an ordinary first-order phase transition both nuclear and quark matter are assumed to be separately electrically neutral, and at some pressure P_0 , corresponding to the coexistence of the two phases, their baryon chemical potentials are equal, i.e.,

$$\mu_{NM}(P_0) = \mu_{QM}(P_0). \quad (17)$$

Such phase transition scenario is known as phase transition with constant pressure (Maxwell construction).

Table 2 represents the parameter sets of the mixed phase both with and without δ -meson field. It is shown that the presence of δ -field alters threshold characteristics of the mixed phase. For $B = 60$ MeV/fm³ the lower threshold parameters, n_N , ε_N , P_N are increased, meanwhile the upper ones n_Q , ε_Q , P_Q are slowly decreased. For $B = 100$ MeV/fm³ this behavior changes to opposite.

In Fig 3 and Fig 4 we plot the EOS of star matter with deconfinement phase transition for two values of bag constant, $B = 60$ MeV/fm³ and $B = 100$ MeV/fm³, respectively. The dotted curves correspond to pure nucleonic and quark matters without any phase transition, while the solid lines correspond to two alternative phase transition scenarios. Open circles show the boundary points of the mixed phase.

In Fig 5 we plot the particle species number densities as a function of baryon density n for Glendenning construction. Quarks appear at the critical density $n_N = 0.241$ fm⁻³. The hadronic matter completely disappears at $n_Q = 1.448$ fm⁻³, where the pure quark phase occurs. Fig 6 show the constituents number density as a function of baryon number density n for $B = 100$ MeV/fm³, when phase transition described according to Maxwell construction. Maxwell construction leads to the appearance of a discontinuity. In this case, the charge neutral nucleonic matter at baryon density $n_1 = 0.475$ fm⁻³ coexisted with the charge neutral quark matter at baryon density $n_2 = 0.650$ fm⁻³. Thus, the density range $n_1 < n < n_2$ is forbidden. In the Maxwell construction case the chemical potential of electrons, μ_e , has a jump at the coexistence

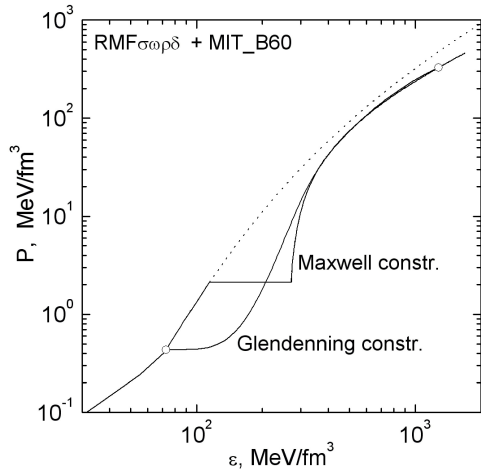


Figure 3: EOS of neutron star matter with the deconfinement phase transition for a bag constant $B = 60 \text{ MeV/fm}^3$. For comparison we plot both the Glendenning and Maxwell constructions. Open circles represent the mixed phase boundaries.

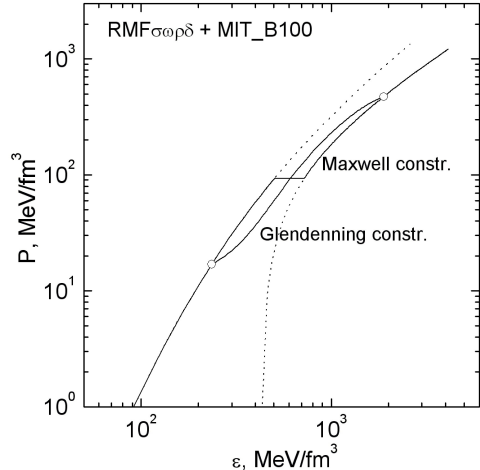


Figure 4: Same as in Fig 3, but for $B = 100 \text{ MeV/fm}^3$.

pressure P_0 . Notice, that such discontinuity behaviour takes place only in usual first-order phase transition, i.e., in the Maxwell construction case.

3 Properties of hybrid stars

Using the EOS obtained in previous section, we calculate the integral and structure characteristics of Neutron stars with quark degrees of freedom.

The hydrostatic equilibrium properties of spherical symmetric and isotropic compact stars in general relativity is described by the Tolman-Oppenheimer-Volkoff(TOV) equations[20]:

$$\frac{dP}{dr} = -\frac{G}{r^2} \frac{(P + \varepsilon)(m + 4\pi r^3 P)}{1 - 2G m/r}, \quad (18)$$

$$\frac{dm}{dr} = 4\pi r^2 \varepsilon, \quad (19)$$

where G is the gravitational constant, r is the distance from the center of star, $P(r)$, $\varepsilon(r)$ are the pressure and energy density at the radius r , respectively, and $m(r)$ is the

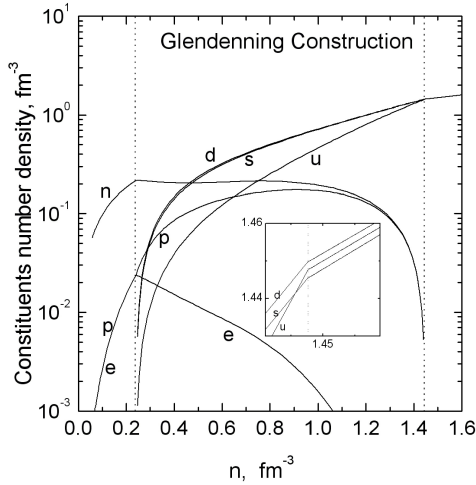


Figure 5: Constituents number density versus baryon number density n for $B = 100 \text{ MeV/fm}^3$ in case of Glendenning construction. Vertical dotted lines represent the mixed phase boundaries.

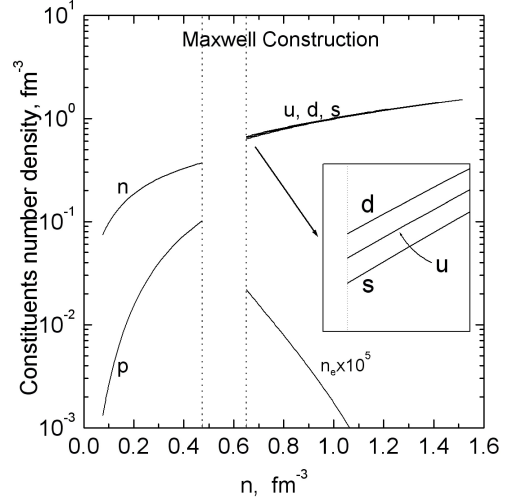


Figure 6: Same as in Fig 5, but for Maxwell construction. Vertical dotted lines represent the density jump boundaries.

mass inside a sphere of radius r . For integration of the TOV equations it is necessary to know the EOS of neutron star matter in a form $\varepsilon(P)$. Using the neutron star matter EOS, obtained in previous section, we have integrated the Tolman-Oppenheimer-Volkoff equations and obtained the gravitational mass M and the radius R of compact stars (with and without quark degrees of freedom) for the different values of central pressure P_c .

Fig 7 and Fig 8 illustrates the $M(R)$ dependence of neutron stars for two values of bag constant $B = 60 \text{ MeV/fm}^3$ and $B = 100 \text{ MeV/fm}^3$, respectively. We can see, that the behaviour of mass-radius dependence significantly differs for two types of phase transitions. Fig 7 shows, that for $B = 60 \text{ MeV/fm}^3$ there are unstable region, where $dM/dP_c < 0$, between two stable branches of compact stars, corresponding to configurations with and without quark matter. In this case, there is a nonzero minimum value of the radius of quark phase core. Accretion of matter on a critical neutron star configuration will then result in a catastrophic rearrangement of the star, forming a star with a quark matter core. The range of mass values for stars, containing the mixed phase, is $[0.085M_\odot; 1.853M_\odot]$ for $B = 60 \text{ MeV/fm}^3$, and is $[0.997M_\odot; 1.780M_\odot]$ for $B = 100 \text{ MeV/fm}^3$. In case of Maxwellian type phase transition the analogous range is $[0.216M_\odot; 1.828M_\odot]$ for $B = 60 \text{ MeV/fm}^3$. From Fig 8 one can observe that when $B = 100 \text{ MeV/fm}^3$, the star configurations with deconfined quark

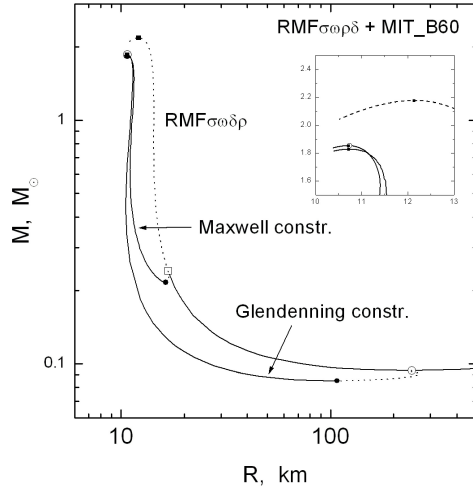


Figure 7: The mass-radius relation of neutron star with different deconfinement phase transition scenarios for bag constant $B = 60 \text{ MeV/fm}^3$. Open circles and squares denote the critical configurations for Glendenning and Maxwellian type transitions, respectively. Solid circles and squares denote hybrid stars with minimal and maximal masses, respectively. .

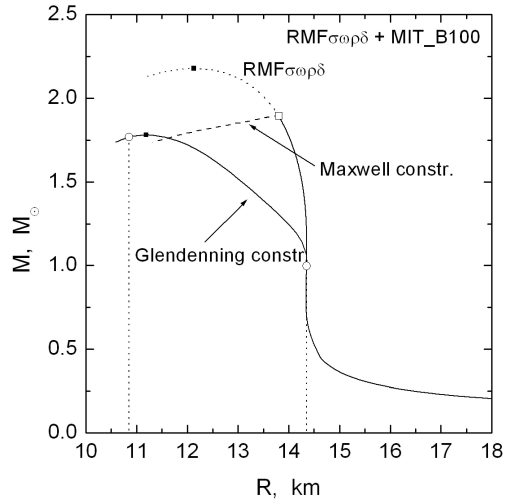


Figure 8: Same as in Fig 7, but for $B = 100 \text{ MeV/fm}^3$.

matter is unstable. Thus, the stable neutron star maximum mass is $1.894M_{\odot}$. Our analysis show, that the pressure upper threshold value for mixed phase is larger, then the pressure, corresponding to maximum mass configuration. This means, that in the model, considered here, the mixed phase can exist in the center of compact stars, but no pure quark matter can exist.

4 Conclusion

In this paper we have studied the deconfinement phase transition of neutron star matter, when the nuclear matter is described in the RMF theory with δ -meson effective fields. We show that the inclusion of scalar isovector δ -meson field terms leads to the stiff nuclear matter EOS. The presence of scalar isovector δ -meson field alters the threshold characteristics of the mixed phase. For $B = 60 \text{ MeV/fm}^3$, the lower threshold parameters, n_N , ε_N , P_N are increased, meanwhile the upper ones, n_Q , ε_Q , P_Q are slowly decreased. For $B = 100 \text{ MeV/fm}^3$ this behavior changes to opposite.

For EOS used in this study, the central pressure of the maximum mass neutron stars is less than the mixed phase upper threshold P_Q . Thus, the corresponding hybrid stars do not contain pure strange quark matter core.

The author would like to thank G.S.Hajyan and Yu.L.Vartanyan for useful discussions on issues related to the subject of this research.

References

- [1] J.D. Walecka, *Ann. Phys.*, **83**, 491 (1974).
- [2] B.D. Serot and J.D. Walecka, in: *Adv. in Nucl. Phys.*, eds. J. W. Negele and E. Vogt, vol. **16** (1986).
- [3] B.D. Serot, J.D. Walecka, *Int.J.Mod.Phys.* **E6**, 515 (1997).
- [4] G.A. Lalazissis, J. Konig, and P. Ring, *Phys.Rev.* **C55**, 540 (1997).
- [5] S. Typel, H.H. Wolter, *Nucl. Phys.* **A656**, 331 (1999).
- [6] C.M. Ko, G.Q. Li, *Journal of Phys.*, **G22**,1673 (1996).
- [7] V. Prassa, G. Ferini, T. Gaitanos, H.H. Wolter, G.A. Lalazissis, and M. Di Toro, arXiv:0704.0554 v1 [nucl-th] (2007)
- [8] H. Miller, B.D. Serot, *Phys. Rev.* **C52**, 2072 (1995).
- [9] S. Kubis, M. Kutschera, *Phys. Lett.*, **B399**,191 (1997).
- [10] B. Liu, V. Greco, V. Baran, M. Colonna, M. Di Toro, *Phys.Rev.* **C65**, 045201 (2002).
- [11] V. Greco, M. Colonna, M. Di Toro, F. Matera, *Phys. Rev.* **C67**, 015203 (2003).
- [12] N.K. Glendenning, *Phys. Rev.* **D 46**, 1274 (1992).
- [13] H. Heiselberg, C.J. Pethick, and E.S. Staubo, *Phys. Rev. Lett.* **70**, 1355 (1993).
H. Heiselberg and M. Hjorth- Jensen, arXiv: 9902033 v1, [nucl-th] (1999).
- [14] G.B. Alaverdyan, *Astrophysics* **52**, 132 (2009).
- [15] G. Baym, H. Bethe, Ch. Pethick, *Nucl.Phys.*, **A175**, 255, 1971.
- [16] N. K. Glendenning, *Compact Stars*, Springer (2000).
- [17] G. B. Alaverdyan, *Gravitation & Cosmology* **15**, 5 (2009).

- [18] A. Chodos, R. L. Jaffe, K. Johnson, C. B. Thorn, V. F. Weisskopf, Phys.Rev.**D9**, 3471 (1974).
- [19] E. Farhi, R. L. Jaffe, Phys.Rev. **D30**, 2379 (1984).
- [20] R. Tolman, Phys.Rev. 55, 364, 1939; J. Oppenheimer and G. Volkoff, Phys.Rev. **55**, 374 (1939).